The Combined Effect of Glycine and Sea-Salt on Aerosol Cloud Droplet Activation Predicted by Molecular Dynamics Simulations.

ARTICLE *in* THE JOURNAL OF PHYSICAL CHEMISTRY A · SEPTEMBER 2013

Impact Factor: 2.69 · DOI: 10.1021/jp407538x · Source: PubMed

5 AUTHORS, INCLUDING:

Thomas Hede
Stockholm University
14 PUBLICATIONS **80** CITATIONS
SEE PROFILE

Yaoquan Tu
KTH Royal Institute of Technology
70 PUBLICATIONS **632** CITATIONS
SEE PROFILE

C. Leck
Stockholm University
148 PUBLICATIONS **3,771** CITATIONS
SEE PROFILE

Hans Agren
KTH Royal Institute of Technology
867 PUBLICATIONS **18,572** CITATIONS
SEE PROFILE

THE JOURNAL OF PHYSICAL CHEMISTRY A

Article

pubs.acs.org/JPCA

Combined Effect of Glycine and Sea Salt on Aerosol Cloud Droplet Activation Predicted by Molecular Dynamics Simulations

Lu Sun,[†] Thomas Hede,[‡] Yaoquan Tu,[†] Caroline Leck,[‡] and Hans Ågren*[,†]

[†]Department of Theoretical Chemistry and Biology, School of Biotechnology, Royal Institute of Technology, S-10691 Stockholm, Sweden

[‡]Department of Meteorology, Stockholm University, S-10691 Stockholm, Sweden

Supporting Information

ABSTRACT: The present study illustrates the combined effect of organic and inorganic compounds on cloud droplet nucleation and activation processes representative for the marine environment. Amino acids and sea salt are common marine cloud condensation nuclei (CCN) which act as a prerequisite for growth of cloud droplets. The chemical and physical properties of these CCN play a key role for interfacial properties such as surface tension, which is important for the optical properties of clouds and for heterogeneous reactions. However, there is a lack of detailed information and in situ measurements of surface tension of such nanosized droplets. Here we present a study of the combined effect of zwitterionic glycine (ZGLY) and sea salt in nanosized water droplets using molecular dynamics simulations, where particular emphasis is placed on the surface tension for the nanosized droplets. The critical supersaturation is estimated by the Köhler equation. It is found that dissolved sea salt interacts with ZGLY through a water bridge and weakens the hydrogen bonds among ZGLYs, which has a significant effect on both surface tension and water vapor supersaturation. Clusters of glycine mixed with sea salt deliquesce more efficiently and have higher growth factors.

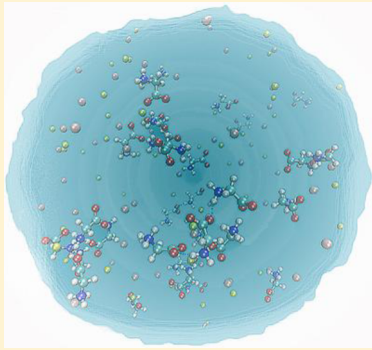

1. INTRODUCTION

Twomey (1974) showed that the state of division of the available water in clouds determines the amount of short-wave radiation scattered back to space, the effect being largest in optically thin clouds with few water drops.[1] The concentration of water drops is largely determined by the concentration of nuclei on which cloud drops can form (cloud condensation nuclei, or CCN). The connection between CCN and cloud albedo has been extended to the remote natural aerosol through the recognition of dimethyl sulfide (DMS) as a potential source of CCN.[2−6] Where do their replacements come from?

Blanchard (1971) and Blanchard and Syzdek (1988) have long advocated that a significant proportion of the remote oceanic aerosol is derived from bubble bursting.[7,8] The bubbles result from entrainment of air induced by wind stress at the air−water interface, which produces primary aerosol particles of CCN sizes. In this process, bubbles scavenge sea salt, debris, and high molecular weight soluble organic surface-active compounds, e.g., dissolved free amino acids, as they rise through the water prior to their injection into the atmosphere.[9,10] Gorzelska et al. measured the amino acid concentration in marine aerosol particles which could reach 10.7 pmol m^{-3}, and Scalabrin et al. recently reported glycine and serotonine to be the most abundant among the amino acids in aerosol particles.[11,12] Measurements have also shown that bubble bursting generated sea salt can contribute a significant fraction of the marine CCN population.[13] The sea salt particles are generally larger than non-sea salt (nss)-sulfate aerosol and have a lower threshold for activation. Hence cloud drops preferentially form on them. The surfactants from soluble organic surface-active compounds scavenged by the bubbles may also influence the water nucleating ability. The particles formed when they burst with laboratory produced particles and with actual atmospheric aerosol have shown that organic surfactants can lower the threshold size for CCN nucleation.[14,15] This would promote cloud droplet growth, which affects the microphysical properties of the cloud so that the reflectivity of the cloud (albedo) is enhanced when the fraction of the population of small droplets is increased.[16]

The activation process of CCN is largely predicted by a traditional equilibrium theory proposed by the Swedish meteorologist Hilding Köhler.[17] The theory consists of the Kelvin effect, which describes the influence on water vapor supersaturation pressure from the curvature of the spherical surface of a droplet, and the Raoult effect, which represents the influence from the solutes. One key parameter in the Kelvin term is the surface tension. The surface tension of an aerosol particle is not only influenced by the curvature of the droplet but also determined by the concentration of amphiphilic solutes.[18] Thus inorganic salt could be assumed to have an increasing effect on surface tension due to the ionic

Received: July 29, 2013
Revised: September 23, 2013
Published: September 24, 2013

interactions, whereas surface-active compounds such as detergents decrease the surface tension due to the amphiphilic properties disturbing the hydrogen bonding at the air/water interface. Laboratory studies of bulk solutions show that the solubility of amino acids changes in salt solutions, and therefore further investigations of mixtures of sea salt and amino acids are required.[19] It still remains a problem, however, to conduct experimental investigations at the nanometer scale potentially important to the early stages of water vapor condensational growth of aerosol particles.

Molecular dynamics (MD) has become a popular approach in a variety of fields, such as nanocluster simulations and interface evaluation, and has been recently shown applicable to mimic atmospheric aerosols by modeling nanosized water solutions and clusters.[20−23] In this study the combined effect of zwitterionic glycine (ZGLY) and sea salt (NaCl) in nanosized water droplets is studied using MD similations. Quantitative data on surface tension, vapor supersaturation, and growth factors for nanosized water droplets (clusters) are calculated and analyzed.

2. COMPUTATIONAL METHODS

Molecular dynamics simulations for a series of a two-system approach, slab and cluster, as listed in Table 1, were carried out with the GROMACS package.[24−27] Throughout the simulations, the concentrations of NaCL and ZGLY in the nanosized water clusters were kept constant: NaCl at 1 mol L^{-1} and ZGLY at 0.56 mol L^{-1}.

To construct the initial configuration, a box with suitable size was first generated, followed by inserting ZGLYs randomly into the box, solvating them with an appropriate number of water molecules, and creating the required number of ions by replacing the same number of water molecules randomly. In order to mimic a planar air/solution interface, the box length along the z axis was extended by an additional 6 nm with the solution placed in the middle of the box. When modeling a droplet (cluster), the system was placed in the center of a new box with each side extended by an additional 6 nm. Simulations were carried out after energy minimization. During the simulations, periodic boundary condition (PBC) was used, and the NVT ensemble was applied with a Nosé−Hoover thermostat to keep the systems at room temperature (298 K).[28,29] The OPLS/AA (optimized potentials for liquid simulation/all-atom) force field together with the modified flexible extended simple point charge model (SPC/E) for water were used to model the interactions between the atoms.[30,31] In the water model, the H−O−H angle bending was modeled by a harmonic potential with the minimal energy at 109.47° and a force constant of 383.0 kJ mol^{-1} rad^{-2}. Bonds containing hydrogen atoms in both water and ZGLYs were constrained by the LINCS algorithm.[32,33] Because the surface tension is very sensitive to the van der Waals interaction, the cutoff radii for both the Coulombic and van der Waals interactions were chosen as 1.5 nm, which have been tested to be sufficient for obtaining the converged surface tension value.[23] The long-range Coulombic interactions were recovered by the PME method .[34,35] Each simulation was conducted for 12 ns with a 2 fs time step of which the first 5 ns concerned equilibration and the later 7 ns was saved every picosecond. For detailed information on how the surface tension is calculated for both planar and curved interfaces, the reader is referred to ref 18.

Table 1. Simulated Systems with Their Number Densities, Equimolar Surface Radii, and Calculated Surface Tension

	Slab System			
	ρ (nm^{-3})	γ_o ($mJ\ m^{-2}$)	γ_d ($mJ\ m^{-2}$)	γ ($mJ\ m^{-2}$)
$1000H_2O$	33.72	62.31	2.57	64.88
$1000H_2O$ + 18NaCl	34.26	64.38	2.68	67.06
$1000H_2O$ + 10GLY	33.29	62.90	2.74	65.64
$1000H_2O$ + 10GLY + 18NaCl	33.65	65.71	2.84	68.55
	Cluster System			
	ρ (nm^{-3})	R_e (nm)	W (10^{-19}J)	γ ($mJ\ m^{-2}$)
$750H_2O$	34.82	1.73	8.70	69.69
1000H2O	34.74	1.90	11.44	75.52
$1500H_2O$	34.63	2.18	15.93	80.12
$2000H_2O$	34.55	2.40	20.13	83.59
$3000H_2O$	34.48	2.75	26.94	85.13
$5000H_2O$	34.33	3.26	39.44	88.39
$1000H_2O$ + 18NaCl	35.23	1.91	13.81	89.95
$2000H_2O$ + 36NaCl	35.06	2.42	25.79	105.45
$3000H_2O$ + 54NaCl	34.91	2.77	34.25	106.59
$5000H_2O$ + 90NaCl	34.85	3.29	49.57	109.60
$1000H_2O$ + 10GLY	33.56	1.93	10.41	66.72
$2000H_2O$ + 20GLY	33.67	2.43	20.02	81.03
$3000H_2O$ + 30GLY	33.74	2.78	27.04	83.64
$5000H_2O$ + 50GLY	33.44	3.30	40.51	88.63
$1000H_2O$ + 10GLY + 18NaCl	34.17	1.94	12.94	82.00
$2000H_2O$ + 20GLY + 36NaCl	34.15	2.45	25.25	100.8
$3000H_2O$ + 30GLY + 54NaCl	34.00	2.80	33.95	103.42
$5000H_2O$ + 50GLY + 90NaCl	34.09	3.32	53.62	116.08

3. RESULTS AND DISCUSSION

The systems simulated are listed in Table 1, together with fitted densities, equimolar surface radii, and calculated surface tensions. Here, we discuss the results for the planar and spherical interfaces.

3.1. Planar Interface. The bulk water is compressed by the two air/water interface and thus has a number density of 33.72 nm^{-3} (corresponding to 1001 kg/m^{-3}). The presence of ZGLYs decreases the density, while the presence of ions increases the density.

The surface tension for a planar interface is determined by the diagonal components of the pressure tensor (P_{zz}, P_{xx}, P_{yy}). With the semiflexible SPC/E water model, the surface tension for a planar water interface is 64.8 $mJ{\cdot}m^{-2}{\cdot}mol^{-1}{\cdot}L$, lower than the experimental value of 72.0 $mJ{\cdot}m^{-2}{\cdot}mol^{-1}{\cdot}L$.[36] After ions were added into the solution, a significant increase of the surface tension was observed as a consequence of the strong electrostatic interaction between the ions and water. Although the nonpolarizable force field used cannot imitate the surface excessive trend of the chloride ions, the surface tension is still accurate. Change of the surface tension with the ion concentration was calculated to be $d\gamma/dC_{ion}$ = 2.18 $mJ{\cdot}m^{-2}{\cdot}mol^{-1}{\cdot}L$, which agrees well with the experimental value of 2.0 $mJ{\cdot}m^{-2}{\cdot}mol^{-1}{\cdot}L$.[37]

The surface tension of the planar ZGLY−water solution is found to increase compared with pure water, and the increment of the surface tension with the concentration is $d\gamma/dC_{gly}$ = 1.36

dx.doi.org/10.1021/jp407538x | J. Phys. Chem. A 2013, 117, 10746−10752

$mJ \cdot m^{-2} \cdot mol^{-1} \cdot L$. This value is slightly overestimated compared with the experimental value of 1.12 $mJ \cdot m^{-2} \cdot mol^{-1} \cdot L$.[38] After sea salt is added into the glycine solution, the ions interact with the ZGLY to increase the surface tension more than a simple addition of the effects from each solute individually.

3.2. Spherical Interface. The clusters are more compact than solutions with a planar interface because they are more compressed by the surface tension. For larger clusters the density gradually decreases and converges to that of the planar solution, because the influence of the surface tension on the inner part of the cluster is reduced as the surface/volume ratio decreases. The density will also change slightly with cutoff radius for the van der Waals interactions.

The surface tension of small clusters was larger than for bulk solution, and we attribute this to the larger surface/volume ratio and more notable interfacial effect. Moreover, this enhancement is augmented further since more pairwise forces orthogonal to the surface (f_k) are involved—both from the increase of the number of molecules and from the decrease of curvature. However, for larger droplets, the reduced surface/volume ratio dominates and the increase in the surface tension is no longer that fast. The surface tension finally approaches that of a planar surface.

The presence of ZGLY in a small cluster reduces the surface tension, indicating that ZGLY facilitates the cluster growth by water vapor condensation. As the cluster grows to the size of 5000 water molecules, our study shows that the surface tension of the ZGLY−water cluster exceeds that of the pure water droplet.

3.3. Structure Analysis. Details from the MD simulations help to explain the properties of mixtures of organic and inorganic compounds. The results show that the distributions of solutes are rather similar between bulk solutions and nanosized droplets. A visual representation for $3000H_2O$ + 30GLY and $3000H_2O$ + 30GLY + 54NaCl is shown in the Supporting Information. Apparently, ZGLYs tend to reside around the center of the cluster. A ZGLY is probable to form hydrogen bonds to another ZGLY independent of ion concentration. A hydrogen bond is defined to be formed when the donor−acceptor distance is less than 3.0 Å, which is the limit of the first solvation shell, and the acceptor−donor-hydrogen angle is limited to 30°. The averaged total number of hydrogen bonds among the ZGLY molecules is 13.5. This number is consistent with the visual representation that a ZGLY has the tendency to form a hydrogen bond with another ZGLY. Hydrogen bonds among ZGLY molecules have an averaged lifetime of about 58 ps and are thus stable considering that the hydrogen bonds between water molecules have an average lifetime of about 1 ps.[39] The number of hydrogen bonds reduces to 11 with ions around ZGLYs, implying that ZGLY is more involved in the solution by the dissolved salt ions. This helps to illustrate the salting-in effect and explains the increased solubility of glycine in sodium chloride solution. The increased involvement of ZGLY with ions sheds light on how ZGLY and ions interact to enhance the surface tension. Nevertheless, no hydrogen bond was found between $-NH_3^+$ of a ZGLY and ions, suggesting that a special ion−zwitterion structure was formed.

In order to better illustrate the ZGLY−ion interaction, a ZGLY was divided into a C-terminal ($-COO^-$) and a N-terminal ($-NH_3^+$). From the radial distribution of the solutes in the cluster (Supporting Information), it can be seen that both ZGLYs and ions tend to reside inside the cluster. This hydrophilic behavior is attributed to the zwitterionic characteristic of the ZGLY with two charged groups and a negligible hydrophobic alkyl group. The methylene group in the middle is small in size and is surrounded by the charged groups, so the hydrophobicity of ZGLY is little affected while the hydrophilicity dominates. The distributions of the C-terminal and N-terminal follow a similar pattern, reflecting no specific orientation for the ZGLY. Moreover, ions are found to exert minor influence on the radial distribution of the ZGLY which indeed are found to be repelled from the interface.

Radial number densities of water molecules, ions, and ZGLYs near the C-terminal and N-terminal of a ZGLY molecule are plotted in Figure 1. The reduced density of ZGLYs near a

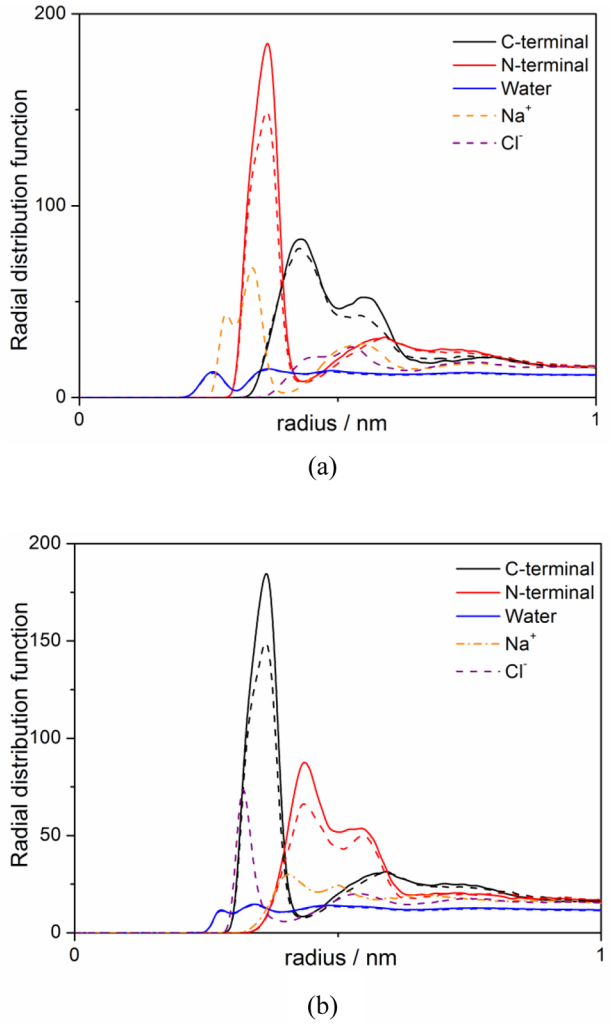

Figure 1. Radial distribution functions of water molecules, ZGLYs, and ions around the (a) C-terminal and (b) N-terminal of a ZGLY. The position of a water molecule is represented by its center of mass. The C-terminal is defined as the C in $-COO^-$ while the N-terminal is defined as the N in $-NH_3^+$. The solid and dashed curves denote systems with and without ions, respectively.

ZGLY also supports the weakened interaction among ZGLYs. Ions do not interact directly with the ZGLY but via a water shell in between them. This explains why there are no hydrogen bonds formed between the ZGLY and salt ions. The water density around the ZGLY is little affected by the ions as the first water shell is limited to 0.3 nm for both terminals. The number

dx.doi.org/10.1021/jp407538x | J. Phys. Chem. A 2013, 117, 10746−10752

of water molecules in the first shell decreases slightly, about 0.3, owing to steric hindrance by the ions.

3.4. Curvature Dependence of the Surface Tension. On the basis of our simulations, we have predicted realistic trends on the curvature dependence of the surface tension. Unfortunately no direct comparison with experimental results is possible as measurements of the surface tension for nanosized clusters are not feasible experimentally. Because the interfacial curvature of a planar interface is zero, it can be treated as the interface of an infinitely large cluster. The surface tension can then be fitted as a polynomial function to the reciprocal of equimolar radius (R_e), as shown in Figure 2.[21] By fixing the intercept before fitting, four polynomial functions are acquired as

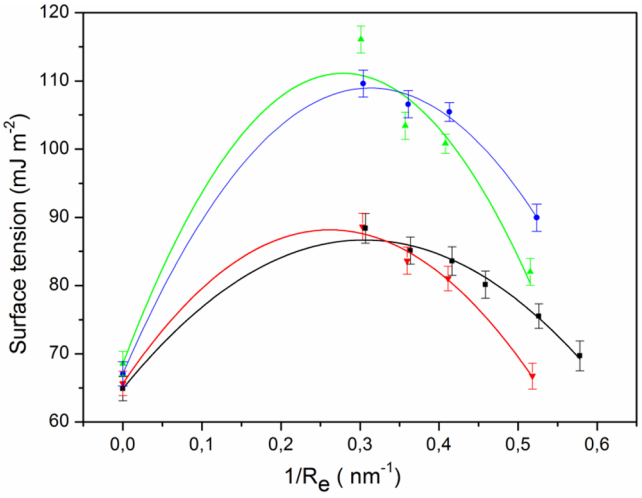

Figure 2. Curvature dependence of the surface tension. The black, red, blue, and green curves represent the fitted curvature dependence of the surface tensions of pure water, salt solution, ZGLY−water, and ZGLY−ion−water system, respectively.

$$\gamma_{water} = 64.88 + 142.85/R_e - 234.04/R_e^2 \quad (1)$$

$$\gamma_{water-ion} = 67.07 + 268.52/R_e - 428.64/R_e^2 \quad (2)$$

$$\gamma_{water-gly} = 65.64 + 172.08/R_e - 328.59/R_e^2 \quad (3)$$

$$\gamma_{water-gly-ion} = 68.55 + 305.62/R_e - 548.54/R_e^2 \quad (4)$$

The above fitted functions describe the surface tension of the water, ion−water, ZGLY−water, and ZGLY−ion−water systems, respectively. The surface tension can be divided into the contributions from water and solutes. The surface-active substance lowers the surface tension exponentially with the increase of its concentration according to the Szyszkowski equation. However, the solutes studied in this work are ions and molecules with two charged groups and therefore interact distinctly with water. In this case, the change of the surface tension with the concentration of the solutes can therefore be thought to be linear. The following functions were derived by separating the contribution of the solutes to the surface tension from water:

$$\gamma'_{water-gly} = \gamma_{water} + (\gamma_{water-gly} - \gamma_{water}) \times C_{gly}/0.56 = \gamma_{water} + (0.76 + 29.23/R_e - 94.55/R_e^2) \times C_{gly}/0.56 \quad (5)$$

$$\gamma'_{water-ion} = \gamma_{water} + (\gamma_{water-ion} - \gamma_{water}) \times C_{ion} = \gamma_{water} + (2.19 + 125.7/R_e - 194.6/R_e^2) \times C_{ion} \quad (6)$$

$$\gamma'_{water-gly-ion} = \gamma'_{water-gly} + (\gamma_{water-gly-ion} - \gamma_{water-gly}) \times C_{ion} = \gamma'_{water-gly} + (2.91 + 133.54/R_e - 199.95/R_e^2) \times C_{ion} \quad (7)$$

Here γ is the fitted surface tension dependent to the curvature, C is the solute concentration, and γ' is the overall surface tension including the water and solute parts. It is worthwhile to notice that for the mixture of glycine and sea salt as solutes, the combined effect is reflected in the ion contribution.

3.5. Supersaturation. With the surface tension obtained, the supersaturation required for droplet activation can be predicted by the modified Köhler equation shown below:

$$S = \frac{P}{P_0} = a_w \exp\left(\frac{4M_w\gamma}{RT\rho d}\right) \quad (8)$$

Here a_w and M_w are the activity and molar mass of water molecules, γ is the surface tension, R is the gas constant, ρ is the solution density, and d is the diameter of the droplet. In this function, the Raoult effect is represented with the water activity. When the solute concentration is low, the activity of water can be believed approximate to the molar fraction expressed as

$$a_w = \frac{n_w}{n_w + \sum \nu_i n_i} \quad (9)$$

where n denotes molar number and ν is the Van't Hoff factor. The subscripts w and i denote water and solutes, respectively.

The surface tension of the water solution calculated from the water model is underestimated compared with the experimental value. Thus, a correction to the surface tension, 6.4 mJ·m^{-2}·mol^{-1}·L, is added to each function. The estimated critical supersaturation is displayed in Figure 3. The parameters used are taken from the experiments by Kristensson, and we use a 50 nm dry glycine particle as nucleus.[40] The computed supersaturation values needed for droplets to grow spontaneously are 0.585%, 0.599%, and 0.603% for the planar water surface tension, curvature-dependent water surface tension, and curvature-dependent surface tension of glycine−waterclusters, respectively. The obtained values are only a little underestimated compared with the experimental value published, which is about 0.6−0.7%. Such a discrepancy is attributed to the fact that the activity of water used in this work was simply evaluated by molar fraction, that the morphology of the solutes was neglected, and that the density of the nuclei used in experiments is uncertain. The wet droplet size at the critical point, in this case, is estimated to be about 240 nm in diameter. At this cluster size, the surface tension enhancement due to

dx.doi.org/10.1021/jp407538x | J. Phys. Chem. A 2013, 117, 10746−10752

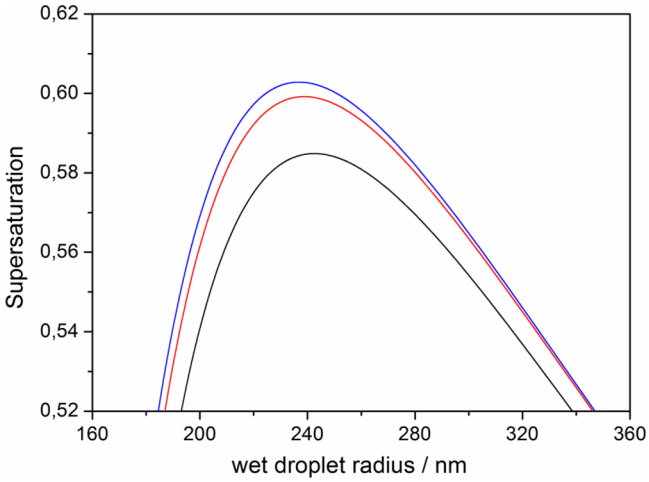

Figure 3. Supersaturation calculated from the Köhler equation (dry glycine particle diameter = 50 nm): (a) the black curve is computed with the surface tension of pure water, 72.4 mJ m^{-2}, (b) the red curve is computed with the curvature dependence of the surface tension corrected, and (c) the blue curve is computed with the influence of ZGLY involved.

curvature is not significant according to the fitted surface tension curves. Consequently, the curvature correction, which makes the results more accurate, is indeed small, but not negligible—0.3 mJ m^{-2} for the surface tension and 0.014% for supersaturation.

The influence of sea salt on the activation of amino acid aerosol particles is also derived by the Köhler equation (eq 8). By adding sea salt to the dry glycine particle with molar ratio to glycine set as 1:10, 1:2, 1:1, 1.8:1, the activation of the droplet becomes more feasible, as presented in Figure 4. The

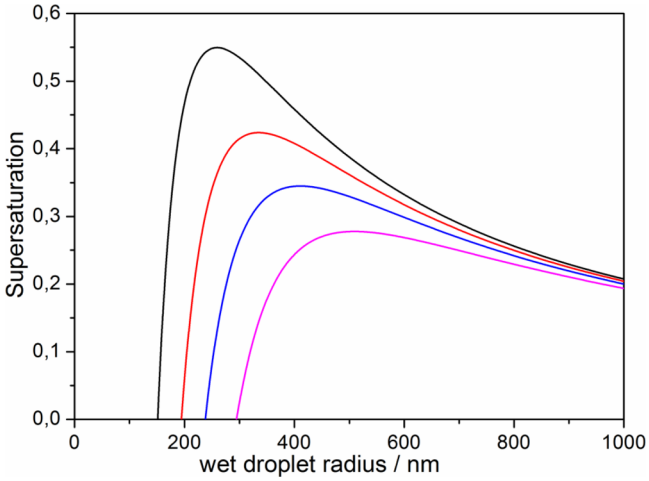

Figure 4. Predicted Köhler curve for glycine−salt mixture (dry glycine particle diameter = 50 nm). Molar proportions between the sea salt and glycine are 1:10, 1:2, 1:1, and 1.8:1, as indicated by the black, red, blue, and purple curves, respectively.

supersaturation can be lowered significantly, from 0.55% to 0.27%, and the preactivation of the droplet increases. Although the surface tension is enhanced with the presence of sea salt ions, this change is mainly owed to the decrease of the activity of water. The Van't Hoff factor for sea salt is 2 as one molecule dissolves into two ions, inducing an evident decrease in water activity.

3.6. Growth Factor. The hygroscopicity of CCNs is important since the initial stage of nucleation is usually a deliquescent transition under subsaturated water vapor conditions. The transition from the crystal to the solvated state is initiated by adsorbing water, and the relative humidity (RH) is thus important. Tang et al. found that a smaller cluster requires higher delinquent RH as the surface tension contributed more to the Gibbs free energy.[41] To characterize the water adsorption during the deliquescent transition, a growth factor (GF) is introduced and defined as the ratio of the diameter of a wet particle after water uptake under certain relative humidity to that of the dry particle:

$$\mathrm{GF} = \frac{d_{\mathrm{wet}}(\mathrm{RH})}{d_{\mathrm{dry}}} \tag{10}$$

Biskos et al carried out experiments on GFs with different sizes of sodium chloride.[42] The GF for 8 nm particles at 80% RH declined to 1.55 from 1.75 for 60 nm particles. This necessitates the application of their model which contains the Kelvin effect, shape factor, and size dependence. The results are depicted in Figure 5. The solid lines are calculated with the fitted surface tension with curvature dependence while the dotted lines are computed with the planar surface tension. The trend agrees well with the experiments.[42] For smaller clusters in Figure 5a, a correction of the curvature dependence is observed although this correction becomes less evident. The size dependence of the GF indicates that a smaller nucleus requires higher RH to obtain the same growth factor as for a larger cluster. The fitted values for small clusters are closer to the experimental ones. For example, in the experiments by Biskos et al, the GFs for 6, 10, and 20 nm dry clusters are 1.43, 1.65, and 1.78 at 85% RH and 1.54, 1.72, and 2.06 at 90% RH, respectively. The GF in the fitted curves for the 6, 10, and 20 nm dry clusters are 1.40, 1.46, and 1.50 at 85% RH and 1.57, 1.65, and 1.71 at 90% RH. The discrepancy for larger sizes is due to the overcorrected size effect. The efficacy of sea salt at the initial growth stage is distinguishably illustrated in Figure 5b. Pure glycine particles will yet deliquesce until the RH reaches as high as 83%. By blending sea salt evenly into a dry glycine particle, the growth becomes more efficient. The RH needed falls below 70%, and the wet particle diameter is 30% larger at an equivalent RH when the molar ratio of sea salt to glycine turns to 1:1.

4. CONCLUSIONS

Reducing the uncertainty in explaining the maintenance of remote marine CCN is apparently a critical element in improving our ability to assess the potential role of aerosols in climate forcing. To improve our understanding of cloud droplet activation and evolution, we need a much better understanding of how the chemistry of the aerosol multiphase system will influence the water nucleating ability of the particles derived from bubble bursting at the air−water interface.

In this study, we applied MD simulations to mixtures of zwitterionic glycine (ZGLY) and NaCl. The results show that ZGLYs have a decreasing effect on the surface tension for particles of sizes below 6 nm in diameter. This in turn has an impact on the early stages of delinquence and water vapor condensation. Ions influence only to a small extent the distribution of ZGLYs in the cluster, due to a weakening of the ZGLY−ZGLY interaction. The ZGLY molecule is more soluble when surrounded by ions, and the interaction with the

dx.doi.org/10.1021/jp407538x | J. Phys. Chem. A 2013, 117, 10746−10752

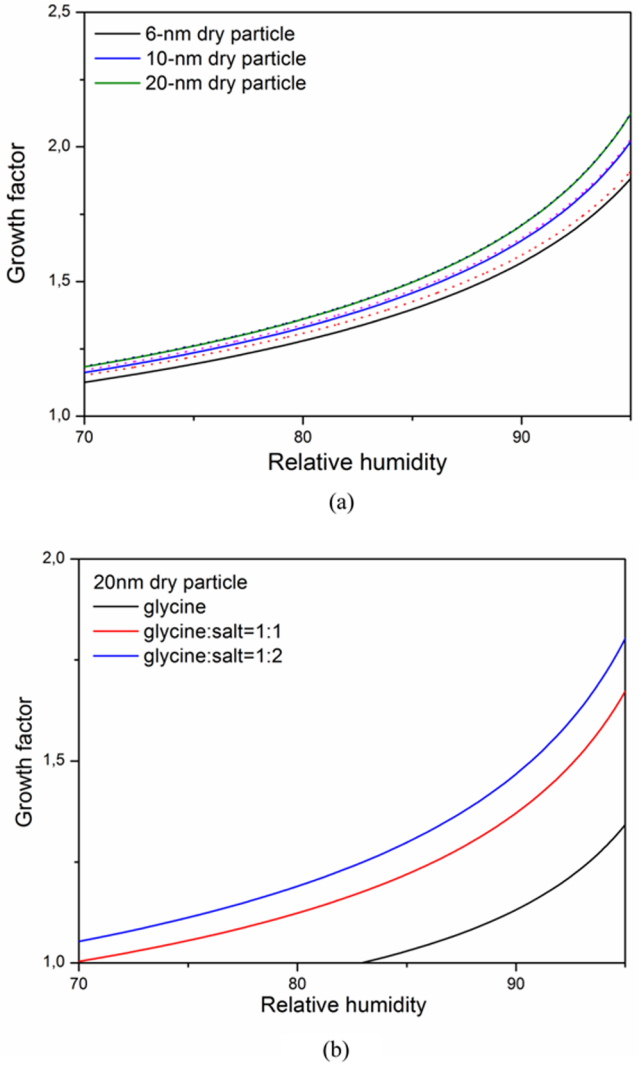

Figure 5. Droplet growth factor: (a) the solid lines are calculated with curvature correction, and the dotted lines are estimated with planar surface tension; (b) growth factor for glycine–salt mixture with different molar ratios.

ions enhances the surface tension. The modeled supersaturation acquired from the Köhler curve for ZGLY is in good accordance with experimental results. The fact that sea salt lowers the critical supersaturation confirms its efficiency in the cloud droplet activation process. Furthermore, the growth factors of sea salt of various sizes are calculated, and it is found that a larger nucleus is beneficial for both initial deliquescence and later growth. Glycine together with sea salt makes the nucleation process much more efficient than this amino acid alone.

In summary, we contend that MD simulations can lead to improved descriptions of atmospheric phenomena at the molecular level motivating further studies of atmospheric relevance with various degrees of sophistication.

■ ASSOCIATED CONTENT

Supporting Information

Radial distribution function of water to a glycine is analyzed to verify that the empirical parameters are able to mimic the hydration structures of a ZGLY; visual configurations from MD simulations are figured to show that ions weaken the hydrogen bonds interaction between ZGLY; number densities of solutes in clusters are plotted to demonstrate that the radial distribution of ZGLY is little affected by ions.This material is available free of charge via the Internet at http://pubs.acs.org.

■ AUTHOR INFORMATION

Corresponding Author

*Phone: +46-855378416. Fax: +46-855378590. E-mail: agren@theochem.kth.se.

Notes

The authors declare no competing financial interest.

■ ACKNOWLEDGMENTS

The authors thank the Swedish Infrastructure Committee (SNIC) for providing computational resources for the project "Multiphysics Modeling of Molecular Materials", SNIC025/12-38. L.S thanks Dr.Li.X. for the discussion during this work.

■ REFERENCES

(1) Twomey, S. Pollution and the Planetary Albedo. *Atmos. Environ.* **1974**, *8*, 1251–1256.
(2) Nguyen, B. C.; Gaudry, A.; Bonsang, B.; Lambert, G. Re-evaluation of the Role Dimethyl Sulfide in the Global Sulphur Budget. *Nature* **1978**, *275*, 637–639.
(3) Charlson, R. J.; Lovelock, J. E.; Andreae, M. O.; Warren, S. G. Oceanic Phytoplankton, Atmospheric Sulphur, Cloud Albedo, and Climate. *Nature* **1987**, *326*, 655–661.
(4) Ayers, G. P.; Gras, J. L. Seasonal Relationship between Cloud Condensation Nuclei and Aerosol Methane Sulphonate in Marine Air. *Nature* **1991**, *353*, 834–835.
(5) Bigg, E. K.; Leck, C. Cloud-Active Particles over the Central Arctic Ocean. *J. Geophys. Res.* **2001**, *106*, 32155–32166.
(6) Leck, C.; Persson, C. Seasonal and Short-Term Variability in Dimethylsulfide, Sulfur Dioxide and Biogenic Sulfur and Sea Salt Aerosol Particles in the Arctic Marine Boundary Layer during Summer and Autumn. *Tellus, Ser. B* **1996**, *48*, 272–299.
(7) Blanchard, D. C. The Oceanic Production of Volatile Cloud Nuclei. *J. Atmos. Sci.* **1971**, *28*, 811–812.
(8) Blanchard, D. C.; Syzdek, L. D. Film Drop Production as a Function of Bubble Size. *J. Geophys. Res.* **1988**, *93*, 3649–3654.
(9) Kuznetsova, M.; Lee, C.; Aller, J. Characterization of the Proteinaceous Matter in Marine Aerosols. *Mar. Chem.* **2005**, *96*, 359–377.
(10) Gershey, R. M. Characterization of Seawater Organic Matter Carried by Bubble-Generated Aerosols. *Limnol. Oceanogr.* **1983**, *28*, 309–319.
(11) Gorzelska, K.; Galloway, J. N. Amine Nitrogen in the Atmospheric Environment over the North Atlantic Ocean. *Global Biogeochem. Cycles* **1990**, *4*, 309–333.
(12) Scalabrin, E.; Zangrando, R.; Barbaro, E.; Kehrwald, N. M.; Gabrieli, J.; Barbante, C.; Gambaro, A. Amino Acids in Arctic Aerosols. *Atmos. Chem. Phys.* **2012**, *12*, 10453–10463.
(13) O'Dowd, C. D.; Lowe, J. A.; Smith, M. H. Coupling Sea-Salt and Sulphate Interactions and Its Impact on Cloud Droplet Concentration Predictions. *Geophys. Res. Lett.* **1999**, *26*, 1311–1314.
(14) Shulman, M. L.; Jacobson, M. C.; Charlson, R. J.; Synovec, R. E.; Young, T. E. Dissolution Behaviour and Surface Tension Effects of Organic Compounds in Nucleating Cloud Droplets. *Geophys. Res. Lett.* **1996**, *23*, 277–280.
(15) Facchini, M. C.; Mircea, M.; Fuzzi, S.; Charlson, R. J. Cloud Albedo Enhancement by Surface-Active Organic Solutes in Growing Droplets. *Nature* **1999**, *401*, 257–259.
(16) Twomey, S. J. Influence of Pollution on Shortwave Albedo of Clouds. *Atmos. Sci.* **1977**, *34*, 1149–1152.
(17) Köhler, H. T. The Nucleus in and the Growth of Hygroscopic Droplets. *Faraday Soc.* **1936**, *32*, 1152–1161.

(18) Li, X.; Hede, T.; Tu, T.; Leck, C.; Ågren, H. Surface-Active cis-Pinonic Acid in Atmospheric Droplets: A Molecular Dynamics Study. *J. Phys. Chem. Lett.* **2010**, *1*, 769−773.
(19) Khoshkbarchi, M. K.; Vera, J. H. Effect of NaCl and KCl on the Solubility of Amino Acids in Aqueous Solutions at 298.2 K: Measurements and Modeling. *Ind. Eng. Chem. Res.* **1997**, *36*, 2445−2451.
(20) Alejandre, J.; Tildesley, D. J.; Chapela, G. A. Molecular-Dynamics Simulation of the Orthobaric Densities and Surface-Tension of Water. *J. Chem. Phys.* **1995**, *102*, 4574−4583.
(21) Li, X.; Hede, T.; Tu, Y.; Leck, C.; Ågren, H. Glycine in Aerosol Water Droplets: A Critical Assessment of Kohler Theory by Predicting Surface Tension from Molecular Dynamics Simulations. *Atmos. Chem. Phys.* **2011**, *11*, 519−527.
(22) Hede, T.; Li, X.; Leck, C.; Tu, Y.; Ågren, H. Model HULIS Compounds in Nanoaerosol Clusters—Investigations of Surface Tension and Aggregate Formation Using Molecular Dynamics Simulations. *Atmos. Chem. Phys.* **2011**, *11*, 6549−6557.
(23) Sun, L.; Li, X.; Hede, T.; Tu, Y.; Leck, C.; Ågren, H. Molecular Dynamics Simulations of the Surface Tension and Structure of Salt Solutions and Clusters. *J. Phys. Chem. B* **2012**, *116*, 3198−3204.
(24) Berendsen, H. J. C.; van der Spoel, D.; van Drunen, R. Gromacs—A Message-Passing Parallel Molecular-Dynamics Implementation. *Comput. Phys. Commun.* **1995**, *91*, 43−56.
(25) Hess, B.; Kutzner, C.; van der Spoel, D.; Lindahl, E. Algorithms for Highly Efficient, Load-Balanced, and Scalable Molecular Simulation. *J. Chem. Theory. Comput.* **2008**, *4*, 435−447.
(26) Lindahl, E.; Hess, B.; van der Spoel, D. GROMACS 3.0: A Package for Molecular Simulation and Trajectory Analysis. *J. Mol. Model.* **2001**, *7*, 306−317.
(27) van der Spoel, D.; Lindahl, E.; Hess, B.; Groenhof, G.; Mark, A. E.; Berendsen, H. J. C. GROMACS: Fast, Flexible, and Free. *J. Comput. Chem.* **2005**, *26*, 1701−1719.
(28) Nosé, S. A Molecular-Dynamics Method for Simulations in the Canonical Ensemble. *Mol. Phys.* **1984**, *52*, 255−268.
(29) Hoover, W. G. Canonical Dynamics−Equilibrium Phase-Space Distributions. *Phys. Rev. A* **1985**, *31*, 1695−1697.
(30) Jorgensen, W. L.; Maxwell, D. S.; Tirado-Rives, J. Development and Testing of the OPLS All-Atom Force Field on Conformational Energetics and Properties of Organic Liquids. *J. Am. Chem. Soc.* **1996**, *118*, 11225−11236.
(31) Berendsen, H. J. C.; Grigera, J. R.; Straatsma, T. P. The Missing Term in Effective Pair Potentials. *J. Phys. Chem.* **1987**, *91*, 6269−6271.
(32) Hess, B.; Bekker, H.; Berendsen, H. J. C.; Fraaije, J. G. E. M. LINCS: A Linear Constraint Solver for Molecular Simulations. *J. Comput. Chem.* **1997**, *18*, 1463−1472.
(33) Hess, B. A. Parallel Linear Constraint Solver for Molecular Simulation. *J. Chem. Theory Comput.* **2008**, *4*, 116−122.
(34) Darden, T.; York, D.; Pedersen, L. Particle Mesh Ewald—An N·Log(N) Method for Ewald Sums in Large Systems. *J. Chem. Phys.* **1993**, *98*, 10089−10092.
(35) Essmann, U.; Perera, L.; Berkowitz, M. L.; Darden, T.; Lee, H.; Pedersen, L. G. A Smooth Particle Mesh Ewald Method. *J. Chem. Phys.* **1995**, *103*, 8577−8592.
(36) Lide, D. R.; Frederikse, H. P. R. *CRC Handbook of Chemistry and Physics*, 79 ed.; CRC Press: Baco Raton, FL, 1998.
(37) Washburn, E. W. *International Critical Tables of Numerical Data Physics,Chemistry, and Technology*; McGraw-Hill: New York, 1928.
(38) Bull, H. B.; Breese, K. Surface Tension of Amino Acid Solutions: A Hydrophobicity Scale of the Amino Acid Residues. *Arch. Biochem. Biophys.* **1974**, *161*, 665−670.
(39) Keutsch, F. N.; Saykally, R. J. Water Clusters: Untangling the Mysteries of the Liquid, One Molecule at a Time. *Proc. Natl. Acad. Sci.* **2001**, *98*, 10533−10540.
(40) Kristensson, A.; Rosenorn, T.; Bilde, M. Cloud Droplet Activation of Amino Acid Aerosol Particles. *J. Phys. Chem. A* **2010**, *114*, 379−386.
(41) Tang, I. N.; Munkelwitz, H. R. Composition and Temperature-Dependence of the Deliquescence Properties of Hygroscopic Aerosols. *Atmos. Environ.* **1993**, *27*, 467−473.
(42) Biskos, G.; Russell, M.; Buseck, P. R.; Martin, S. T. Nanosize Effect on the Hygroscopic Growth Factor of Aerosol Particles. *Geophys. Res. Lett.* **2006**, *33*, L07801.